9. Projectile ❖ ❖ ❖

Meteoritic remnants of the impacting asteroid that produced Barringer Crater littered the landscape when exploration began ~115 years ago. As described in Chapter 1, meteoritic irons are what initially captured Foote's interest and spurred Barringer's interest in a possibly rich natural source of native metal. After Foote's description was published, samples were collected by F. W. Volz at a nearby trading post and sold widely. Gilbert (1896) estimated that 10 tons of meteoritic debris had already been recovered by the time of his visit. Similarly, Barringer (1905) estimated that 10 to 15 tons of it were circulating around the world by the time his exploration work began. Fortunately, he tried to document the geographic and mass distribution of that debris in a detailed map, which is reproduced in Fig. 9.1. The map indicates that meteoritic irons were recovered from distances approaching 10 km. Gilbert (1896) apparently recovered a sample nearly 13 km beyond the crater rim. A lot of the meteoritic material was oxidized. It is sometimes simply called oxidized iron, but large masses are also called shale balls. A concentrated deposit of small oxidized iron fragments was found northeast of the crater, although those types of fragments are distributed in all directions around the crater. The current estimate of the recovered meteoritic iron mass is 30 tons (Nininger, 1949; Grady, 2000), although this is a highly uncertain number. Specimens were transported in pre-historical times and have been found scattered throughout Arizona (see, for example, Wasson, 1968). Specimens have also been illicitly removed in recent times, without any documentation of the locations or masses recovered.

These iron fragments are collectively called the Canyon Diablo meteorite, whose namesake is a sinuous canyon west of the crater. This meteorite is a coarse octahedrite (Fig. 9.2) with a bandwidth of 1.2 to 2.2 mm. It is chemically classified as a Group IAB iron. This is a non-magmatic type of iron meteorite. Intriguingly, the IAB irons appear to have been produced in impact craters on at least two early solar system planetesimals. Collisions between planetesimals produced impact melt pools that differentiated (Goldstein *et al.*, 2014; Worsham *et al.*, 2017), allowing the denser metal and sulfide components to sink and, thus, collate into significant volumes. Based on the cooling rates of the iron meteorites, I estimate the craters were 150 to 300 km in diameter on planetesimals >300 km diameter. At some later date, the planetesimals were disrupted, producing iron metal-dominated asteroids, one of which eventually collided with Earth to produce Barringer Meteorite Crater.

The asteroid was dominated by Fe,Ni-alloys, particularly kamacite, reflecting a bulk chemical composition with 6.91 to 7.10 wt% Ni (Moore *et al.*, 1967; Wasson and Ouyang, 1990). The mineralogical diversity, however, is large (Table 9.1), and growing as new techniques identify nanoparticle inclusions composed of platinum group elements, transition metal-rich nitrides, and other phases (Garvie, 2017). As noted in Chapter 1, diamond is one of the mineralogical components of Canyon Diablo specimens. The interpretation of the diamond-bearing specimens led to a firestorm of controversy. Urey (1956) suggested the diamonds were produced in hydrostatic equilibrium and, thus, came from a planet of sufficient size to produce very high pressures. That implies a planetesimal in excess of 2020 km. Indeed, on the basis of diamonds, Urey postulated a series of Moon-sized bodies as the source of meteoritic material. Lipschutz and Anders (1961a,b) correctly argued that the diamonds were formed from carbon-graphite-troilite nodules by high shock pressures generated by the impact. Not everybody was immediately convinced. Carter and Kennedy (1964) were critical, which generated an interesting exchange (Anders and Lipschutz, 1966). The diamonds also caused a brief public sensation when the size of the diamond(s) was errantly equated with that of asteroid. One newspaper (The Indianapolis Star, Sunday, October 6, 1912, page 3) headline read: "Syndicate of Mining Men Sink Shaft in Search for Diamond Half Mile Thick." The article goes on to say "But the most remarkable thing

about this meteorite, apart from its prodigious size, is that fact that in all probability it consists of one huge diamond."

Some of the carbon-graphite-troilite nodules are cross-cut with veins of metal (Fig. 9.2). It has long been wondered how those veins were produced. Were they a product of the original differentiation and crystallization processes that occurred in a planetesimal crater where the iron formed? Were they the product of impact-remobilization of melt in an event that occurred soon after solidification? Or were they the product of a much younger impact event during the evolution of the planetesimal as it evolved into a near-Earth asteroid that hit Earth? New analytical techniques were recently applied to the metal in one of those graphite nodules to answer that question (Hilton *et al.*, 2017). That study found that the veins have a composition that falls parallel to a primordial Re-Os isochron, suggesting the veins formed during an early event in solar system history. Highly siderophile element abundances in kamacite in the vein, when normalized to abundances in kamacite in the bulk Canyon Diablo meteorite, correlate with partition coefficient, suggesting the vein formed by partial melting of the Canyon Diablo host. Thus, the veined graphite nodules are ancient, not a later evolutionary product.

An analysis of meteorites from the crater rim and surrounding plain (Fig. 9.3) indicated the rim samples are much more strongly reheated than the plain samples and saw much higher shock pressures. Thus, the diamond-bearing specimens are concentrated on the crater rim (Nininger, 1956; Moore *et al.*, 1967). Heymann *et al*. (1966) conducted a detailed study of 56 Canyon Diablo specimens distributed from the crater rim to distances of about 4 mi (6½ km) and used cosmogenic nuclides to determine their original depth in the parent asteroid. Moderately- to severely-shocked specimens came from greater depths (*e.g.*, a mean of 132 cm *vs* 72 cm). Diamond-bearing and rim specimens came from greater mean depths (135 and 127 cm, respectively) than plains specimens (81 cm). They noted that the severely shocked specimens were recovered on top of the NE and SE portions of the continuous ejecta blanket, suggesting a ray-like distribution pattern and preferential distribution of material from slightly deeper levels of the asteroid in those directions.

Table 9.1. Minerals in the Canyon Diablo Meteorite

Mineral Name	Chemical Formula	Type of Mineral
kamacite	Fe,Ni-alloy	metal
taenite	Fe,Ni-alloy	metal
troilite	FeS	sulfide
daubreelite	$FeCr_2S_4$	sulfide
sphalerite	(Fe,Zn)S	sulfide
mackinawite	$(Fe,Ni)S_{0.9}$	sulfide
chalcopyrrhotite	(Cu,Fe)S	sulfide
schreibersite	$(Fe,Ni)_3P$	phosphide
cohenite	$(Fe,Ni,Co)_3C$	carbide
haxonite	$(Fe,Ni)_{23}C_6$	carbide
graphite	C	carbon
diamond	C	carbon
lonsdaleite	C	carbon
olivine	$(Mg,Fe)_2SiO_4$	silicate
pyroxene	$(Mg,Fe,Ca)_2Si_2O_6$	silicate
plagioclase	$(Ca,Na)(Si,Al)_4O_8$	silicate
ureyite	$NaCrSi_2O_6$	silicate
krinovite	$NaMg_2Cr_2Si_3O_{10}$	silicate
chromite	$FeCr_2O_4$	oxide
rutile	TiO_2	oxide

Additional details about the Canyon Diablo meteorite appear in V.F. Buchwald's volumes about iron meteorites (1975).

In addition to meteoritic fragments, isolated opaque melt droplets were showered around the crater, either as a direct impact melt product or as a molten condensate from an impact-generated vapor cloud. In an early survey, Nininger (1951) reported a recovery rate of 100 g/ft^3 of ejecta and/or alluvium derived from ejecta, which is 3,000 tons of spherules per square mile. He says the total area covered by the spherules is unclear, although there is a "sparse sprinkling...over 100 sq mi." Nininger (1956) later amended these estimates, reporting that 4,000 to 8,000 tons of spherules exist in the upper 4 innches of soil, based on measurements in 60 locations. From these data, he suggests the original asteroid had a mass of 100,000 to 200,000 tons. Most of the spherules are found within 1 ½ mi (2.4 km), although they have been found as far away as 5 mi (8 km) from the crater rim.

The spherules do not have the same composition as Canyon Diablo meteorites and were, thus, somehow fractionated during their formation. The compositional disparity was detected by Nininger (1951), who reported spherules with 17% Ni. Blau *et al.* (1973) found that the spherules are also enriched in S and P. They suggested the spherules formed by preferential shock melting of sulfide-rich portions of the asteroid, rather than oxidation of Fe. Using the dimensions of dendritic crystalline texture in the spherules, they calculated that the 1 mm spherules cooled between 500 and 30,000 °C/sec. They further argued that unshocked "plains" specimens spalled off the asteroid as it approached the surface, that shocked "rim" specimens were blasted off the trailing edge or backside of the asteroid, and that the remainder of the asteroid was dispersed in vapor cloud.

More recently, cosmogenic nuclides have been used to determine the source depths of the spherules on the asteroid. Surprisingly, this signature is preserved, despite the fractionation of the principal siderophile elements. Xue *et al.* (1995) examined the cosmogenic nuclides ^{10}Be and ^{26}Al in 17 spherules and compared them to meteorite fragments. They concluded that the spherules come from a greater depth than meteorites (or that Al and Be is lost during the spherule-forming process). Leya *et al.* (2002) pursued more cosmogenic noble gases. They also concluded that the spheroids come from a deeper depth than meteorites, but still from within a distance of 2.3 m from the pre-atmospheric asteroid surface.

Other isotope systems were employed to independently assess the relative depths of meteorite and spherule production. Schnabel *et al.* (1999) found that a group of spherules contains 7 times less ^{59}Ni than meteorite specimens, implying the spherules came from a depth that is 0.5 to 1.0 m deeper in the impactor than the meteorites. In absolute terms, their results suggest the spherules came from a region that was 1.3 to 1.6 m beneath the pre-atmospheric surface. A model simulation of the impact event in that same study suggested that 1.5 to 2 m of the backside of asteroid (assuming spherical symmetry, 30 m diameter asteroid, and a 20 km/s impact velocity) survives as solid material. This represents 16% of asteroid. The remainder was obliterated and these authors suggest that the bulk of that material was dispersed in a spray of fine molten material and did not involve a significant vapor component. They also argued that the Ni isotope data are consistent with 20 km/s impact simulation, not a slower, 15 km/s simulation; I refer the reader to their paper for details of that discussion.

A crude schematic of the asteroid that summarizes these data is shown in Fig. 9.4. The schematic diagram illustrates a perfectly spherical asteroid. In reality, the asteroid probably had an irregular surface and may have been significantly elongated. To illustrate a possible morphology, model images based on radar data are also included in Fig. 9.4 courtesy of the late Steve Ostro. The model images are of near-Earth asteroid (29075) 1950 DA, which is a suspected metallic asteroid that may pass close by Earth in 2880 and may have a probability of impact as high as 1/300 (Busch *et al*., 2007). These images were selected rather than those of metallic main belt asteroids, because the Canyon Diablo asteroid was truly a

near-Earth asteroid. The other candidate near-Earth metallic asteroid that has been imaged with radar is 1986 DA (Ostro *et al.*, 1991). Two previously imaged metallic asteroids in the main asteroid belt are 216 Kleopatra and 16 Psyche. NASA has recently approved a spacecraft mission to the asteroid 16 Psyche.

As the model images suggest, metallic asteroids can have irregular surfaces that reflect their collisional evolution. In the case of the Canyon Diablo asteroid, cosmic ray exposure ages suggest the object was liberated in a planetesimal breakup event ~540 million years ago and was subsequently involved in a secondary collision ~170 million years ago (Heymann *et al.*, 1966; Michlovich *et al*., 1994).

It is not yet clear how surface irregularities or the shape of the asteroid may have affected the excavation of the crater and distribution of debris around the crater (including the distribution of projectile components). This is an area of study that has become approachable only recently with the advent of new computational codes that permit 3-D simulations with asymmetrical components.

The size of (29075) 1950 DA is ~ 1 km in diameter, which is far larger than the Canyon Diablo asteroid. Previous estimates of its diameter generally fall within the range of 10 to 50 m, but the exact size is still uncertain. To help readers link a discussion of proposed masses with asteroid diameters, I built a table (Table 9.2) of hypothetical spherical projectiles with radii from 10 to 25 m (and, thus, diameters of 20 to 50 m). As noted above, a recent simulation of the impact event assumed a 30 m diameter object, which corresponds to a mass of 1.1×10^8 kg or 110,000 metric tons assuming a density of 7.8 g/cm^3. The most recent simulation favored a ~42 m diameter object with a mass of ~3.2×10^8 kg (Collins *et al.*, 2016). Other mass estimates include 400,000 tons (Magie, 1910); 10,000,000 tons (Barringer, 1914); 5,000 to 3,000,000 tons (Moulton, 1931; per Hoyt, 1987); 15,000 tons (Wylie, 1943a,b); 5,000,000 tons (Öpik, 1936; Rostoker, 1953); 100,000 to 200,000 tons (Nininger, 1956); 2,600,000 tons (Öpik, 1958); 30,000 to 194,000 tons (Bjork, 1961); 63,000 tons (corresponding to 25 m sphere; Shoemaker, 1963); and 500,000 to 1,000,000 tons (Shoemaker in Elston, 1990), as discussed in greater detail by Buchwald (1975) and Hoyt (1987). Only a small fraction of this mass survives. As described above, the current estimate of surviving meteoritic material is 30 tons. In addition, Rinehart (1958) estimates 8,000 tons survives as dispersed metallic particles.

The fate of the missing material has been at the center of considerable debate. Barringer, of course, thought it was buried beneath the crater floor. He considered the alternative possibility that the object was vaporized (Barringer, 1910). In that case, he reasoned, the vaporized projectile and target materials would have re-condensed, producing a mass of material (perhaps similar to rock flour) that was stained with iron and nickel oxides. Since this is not observed, he argued the mass must still exist inside the crater. (At this point in the development of his model, he also thought the asteroid was a cluster of fragments rather than a solid mass.)

Others have argued that a large fraction of the object was obliterated, either in the form of a vapor or finely-dispersed molten mist. A quantitative assessment of that fraction and the amount of obliterated material that was truly ejected is still lacking. Or, rather, a consensus has not developed around one of the proposed answers. Shoemaker, for example, maintained that one-third to one-half of the projectile mass is dispersed in material that remains in the crater (Elston, 1990), consistent with his initial assessment of the impact event (Shoemaker, 1963). In contrast, others have suggested nearly all of the projectile was dispersed beyond the rim of the crater as melted and/or vaporized ejecta (*e.g.*, Blau *et al.*, 1973).

The size and strength of the Canyon Diablo asteroid affected the outcome of the impact event. Smaller and weaker objects are often unable to penetrate the atmosphere without catastrophically

Table 9.2. Masses of hypothetical iron asteroids

Radius (m)	Volume (m^3)	Density (g/cm^3)	Mass (kg)	Mass (metric ton)
10	4189	7.8	3.27×10^7	3.27×10^4
11	5575	7.8	4.35×10^7	4.35×10^4
12	7238	7.8	5.65×10^7	5.65×10^4
13	9203	7.8	7.18×10^7	7.18×10^4
14	11494	7.8	8.97×10^7	8.97×10^4
15	14137	7.8	1.10×10^8	1.10×10^5
16	17157	7.8	1.34×10^8	1.34×10^5
17	20580	7.8	1.61×10^8	1.61×10^5
18	24429	7.8	1.91×10^8	1.91×10^5
19	28731	7.8	2.24×10^8	2.24×10^5
20	33510	7.8	2.61×10^8	2.61×10^5
21	38792	7.8	3.03×10^8	3.03×10^5
22	44602	7.8	3.48×10^8	3.48×10^5
23	50965	7.8	3.98×10^8	3.98×10^5
24	57906	7.8	4.52×10^8	4.52×10^5
25	65450	7.8	5.11×10^8	5.11×10^5

fragmenting far above the ground. For example, a 6 to 8 m diameter stony asteroid with L-chondrite affinities fell about ~15,000 years ago in northern Arizona, but fragmented into thousands of stones (the Gold Basin meteorites) that showered more than 225 km^2 of the Earth's surface rather than create a hypervelocity impact crater (Kring *et al*., 2001). In the case of Barringer Crater, however, the asteroid was able to collide with the Earth's surface while still moving with a large fraction of its cosmic velocity.

When discussing the size of near-Earth asteroids like the one that produced Barringer Crater, it is also important to keep the density of the objects in mind. For example, when an L-chondrite asteroid exploded near the Russian town Chelyabinsk in 2013, it was often described as being half that of the asteroid that produced the ~1 km crater in Arizona. However, the size of that object (~20 m diameter) relative to the size of the Canyon Diablo asteroid (~40 m diameter) is an incomplete comparison. Because the Canyon Diablo asteroid was denser, it had ~28 times more mass and, thus, was ~28 times more explosive than the Chelyabinsk event (Fig. 9.5)

As noted briefly above, Barringer wondered whether the impacting asteroid hit as a solid iron mass, a cluster of iron fragments, or as iron fragments within a stony or icy matrix. The impact cratering community continues to debate the first two options. Results are in considerable flux at the moment, so I will not try to capture them here and suggest instead that interested students watch the literature.

With regard to Barringer Crater and the projectile that produced it, there are two other observations worth noting. First, with a diameter of ~1 km, the crater approaches the lower limit of hypervelocity craters on Earth (Table 9.3). The atmosphere screens most objects that make smaller craters. That is, the atmosphere shields the surface from objects that are smaller or weaker. Because most small craters are associated with iron asteroids, they appear to be stronger than stony asteroids. Second, the number of craters produced by type IAB irons, relative to other irons, is higher than the ratio of those objects seen in the smaller meteorite population. At least 16 to 17 of the craters in Table 9.3 were generated by irons and, of these, 6 (or ~35%) were produced by type IAB irons. Also, at least 24% of all the small crater impacts were produced by type IAB iron asteroids. In contrast, only 10% of observed iron meteorite falls are type IAB (Grady, 2000). Even in a combined population of iron meteorite finds and falls, type IAB specimens constitute only 15% of the population. The data suggest one of three conclusions: (1) Type

IAB asteroids are stronger than other irons and, thus, better able to penetrate the atmosphere; (2) Type IAB asteroids are less collisionally evolved than other irons and, thus, less populous among meteorite-size objects; or (3) we are falling prey to the vagaries of small number statistics. Because the asteroid that produced Barringer Crater was once part of a larger asteroid that was fragmented, it might be interesting to examine the size distribution of the type IAB asteroids that have hit Earth in the past and infer something about the sizes of type IAB asteroids in that distribution that have either been lost via other processes or still remain in near-Earth space. Thus far, all of the craters unambiguously linked to type IAB impactors are small (<100 m) and young (< 1 Ma). There are suggestions, however, that the ~5 km diameter Gardnos crater, produced at least 385 Ma (Grier *et al.*, 1999), may have been produced by a type IA or IIIC asteroid (Goderis *et al.*, 2009), and that the ~6 km diameter Sääksjärvi crater, produced about 560 Ma, may have been produced by a type IA or IIIC asteroid (Tagle *et al.*, 2009). That data should help assess the collisional evolution of the IAB asteroid that eventually produced Barringer Crater.

Smaller near-Earth asteroids, like the one that produced Barringer Crater, are far more numerous than, say, the asteroid that produced the Chicxulub crater and extinguished most life on Earth 65 million years ago (*e.g.*, Kring, 2007; Schulte *et al.*, 2010; and Kring, 2016 for reviews). Thus, while not as deadly as the dinosaur-killing impact event, Barringer-size impacts occur far more frequently. The detection of those small near-Earth asteroids in space has improved tremendously since the first edition of this guidebook was published. Recently collated data are shown in Fig. 9.6 and 9.7. Thus far, of order 10^3 to 10^4 near-Earth asteroids the size of the Canyon Diablo projectile have been detected. Lurking undiscovered, however, are an estimated million objects.

Table 9.3. Small (≲1 km) diameter impact pits and impact craters.

Crater	Locality	Diameter (km)	Projectile	Age (Ma)
Haviland	Kansas, USA	0.011	Pallasite	0
Carancas	Peru	0.013	H-chondrite	0
Dalgaranga	Western Australia, Australia	0.021	Mesosiderite	0.025
Sikhote Alin	Primorskiy Kray, Russia	0.027	IIAB	0
Whitecourt	Alberta, Canada	0.036	IIIAB	<0.0011
Kamil	East Uweinat, Egypt	0.045	Iron ataxite	<0.005
Campo del Cielo*	Gran Chaco Gualamba, Argentina	0.05	IAB	<0.004
Sobolev	Primorye Territory, Russia	0.053	Iron	0
Veevers	Western Australia, Australia	0.08	IIAB	<1
Ilumetsa	Estonia	0.08	?	>0.002
Wabar*	Rub' al Khali, Saudi Arabia	0.097	IIIAB	0.006 ± 0.002
Morasko*	Poznan, Poland	0.1	IAB	0.01
Kaalijarvi*	Saaremaa, Estonia	0.11	IAB	0.004 ± 0.001
Henbury*	Northern Territory, Australia	0.157	IIIAB	<0.005
Odessa*	Texas, USA	0.168	IAB	0.0635 ± 0.0045
Boxhole	Northern Territory, Australia	0.17	IIIAB	0.03
Macha*	Russia	0.3	Iron	<0.007
Aouelloul	Adrar, Mauritania	0.39	Iron or Pallasite	3.1 ± 0.3
Amguid	Algeria	0.45	?	<0.1
Monturaqui	Antofagasta, Chile	0.46	IAB	<1
Kalkkop	South Africa	0.64	?	<1.8
Målingen	Sweden	0.7	L?	458
Wolfe Creek	Western Australia, Australia	0.87	IIIAB	<0.3
Tswaing	South Africa	1.13	Chondrite	0.220 ± 0.052
Barringer	Arizona, USA	1.19	IAB	0.049 ± 0.003

From Grieve (1991), Grieve *et al*. (1995), Koeberl *et al.* (1988, 1994), Holliday *et al.* (2005), Tancredi *et al.* (2009), Kofman *et al*. (2010), Fazio *et al*. (2014), Ormö *et al.* (2014a,b).
*Crater field; diameter of largest crater listed.

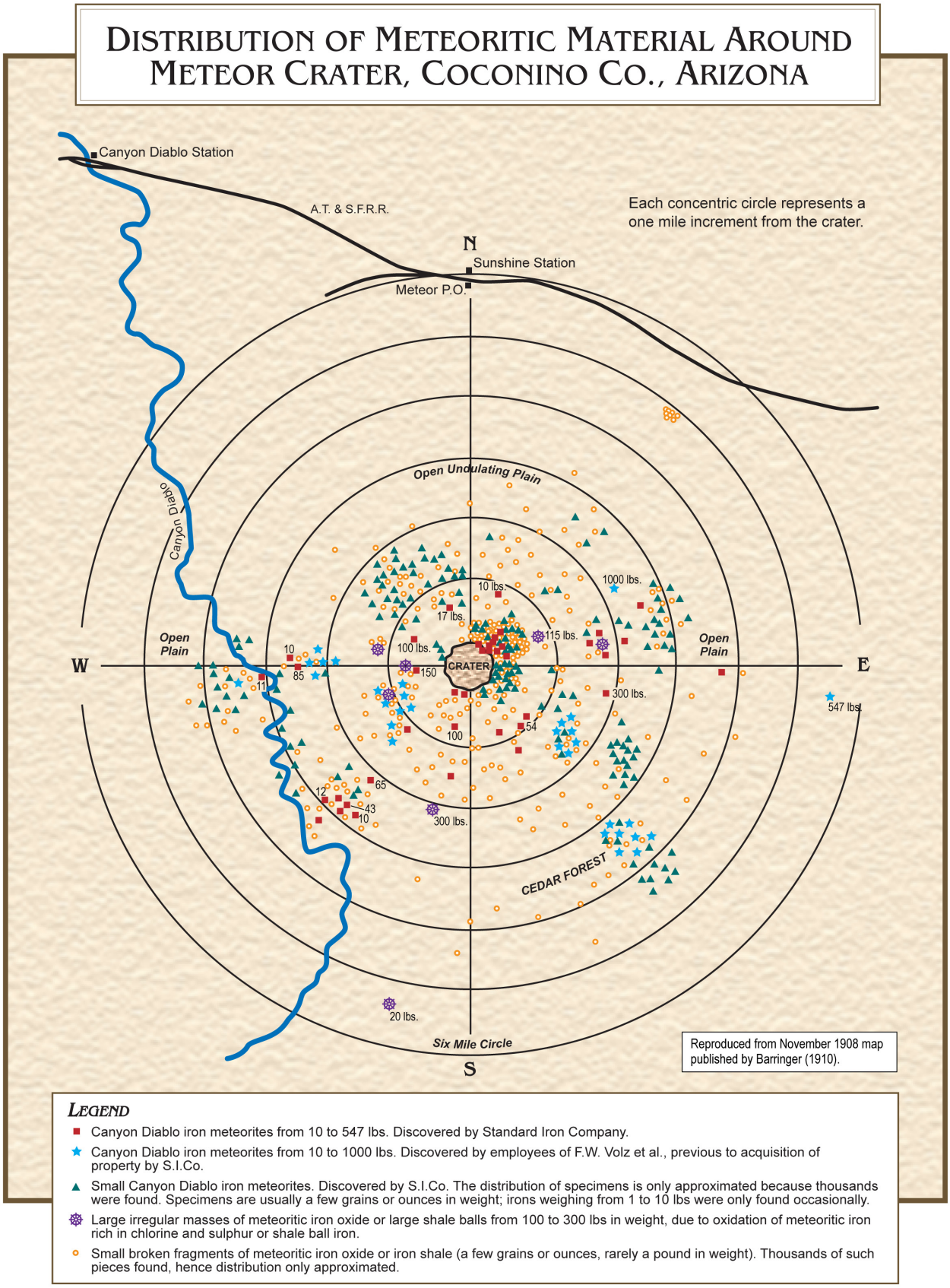

Fig. 9.1. Reproduction of Daniel Moreau Barringer's map of Canyon Diablo meteorite specimens.

Fig. 9.2. Canyon Diablo meteorite. Large fragments of the disrupted iron asteroid were recovered around the crater in the late 1800's and early 1900's as illustrated by a specimen (upper left) in the University of Arizona Mineral Museum, which has material collected when Arizona was still a territory. Etched slices of the meteorite reveal a coarse octahedrite pattern of kamacite and taenite (middle panel with 1-cm cube for scale). This particular slice was taken from a 1,411 g specimen obtained from the descendants of John F. Blandy, the first Arizona Territorial Geologist. Dark troilite and graphite inclusions occur throughout the iron mass and are often rimmed with schreibersite. Some graphite nodules within the meteoritic fragments of the asteroid are cross-cut by veins of metal (lower right, 6-cm-wide specimen).

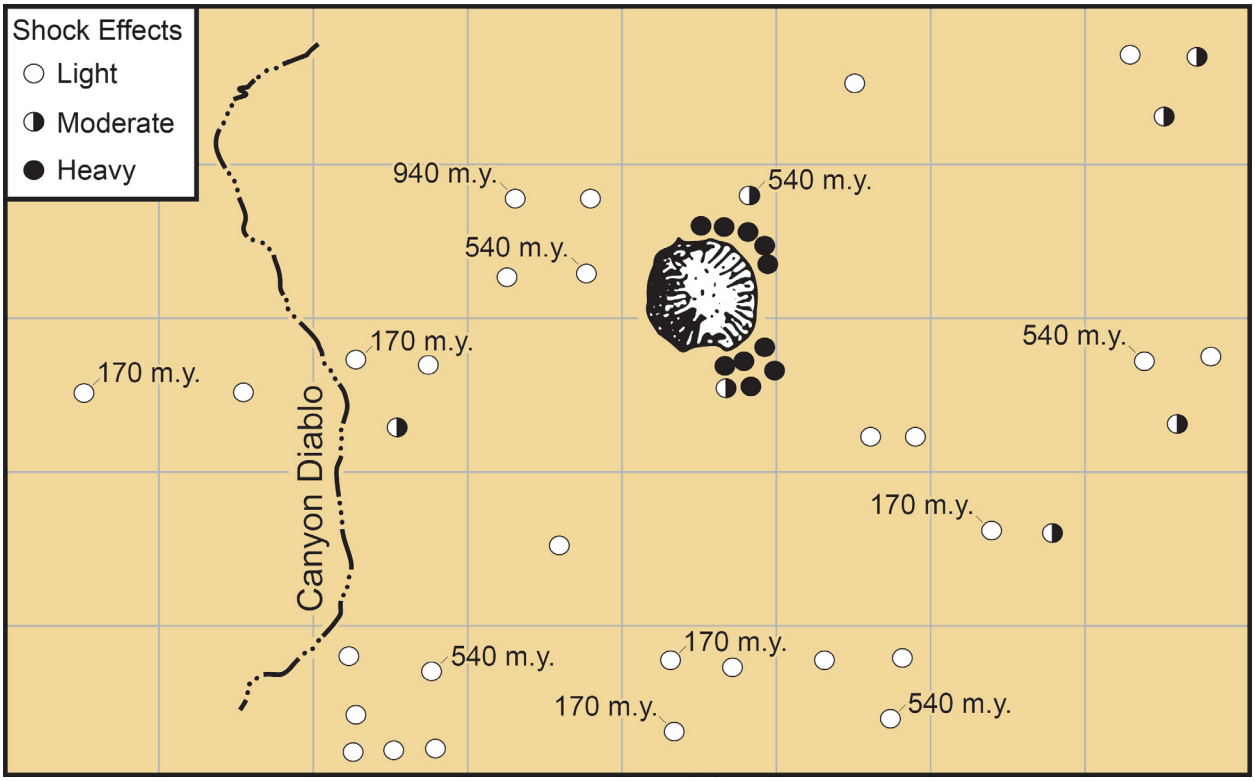

Fig. 9.3. Map of shock effects in rim and plains specimens of Canyon Diablo that were collected in the last century. The specimens with the most severe shock effects were deposited on the crater rim, while low- to moderately-shocked specimens dominated the surrounding plains. Ages reflecting collisional events on the Canyon Diablo asteroid, derived from some of the specimens, are also indicated on the map. (Colorized version of a map published by Heymann *et al.*, 1966.)

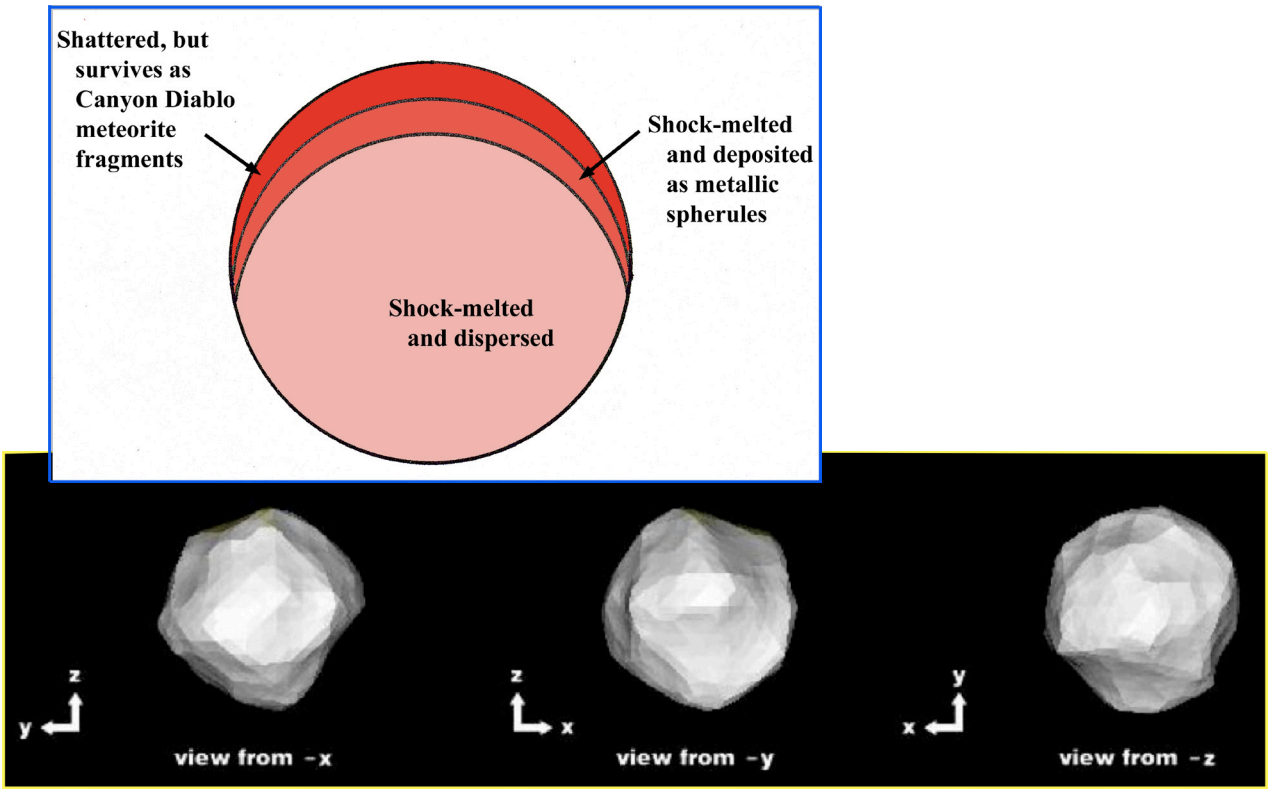

Fig. 9.4. Schematic diagram of the asteroid that produced Barringer Crater (upper left). Cosmogenic nuclides suggest the surviving meteoritic component of the asteroid was derived from a shallower depth (roughly 0.6 to 1.3 m) than molten metallic spherules (roughly 1.3 to 2.0 m depth). Furthermore, lightly-shocked meteorites appear to come from a shallower depth (mean of 0.8 m) than moderately- to heavily-shocked meteorites (mean of 1.3 m depth). The lightly-shocked meteorites are distributed on the plain surrounding the crater, while moderately- to heavily-shocked meteorites are concentrated near the crater rim. Almost all of the diamond-bearing specimens were found on the crater rim. The shape of the asteroid that produced Barringer Crater is unknown, but a suspected metallic near-Earth asteroid is shown (bottom panel) to provide an example of possible morphologies. Three model images based on radar data are shown for (29075) 1950 DA, which were kindly provided by Steve Ostro for our field guide. This object is far larger than the one that produced Barringer Crater (1 km versus 10 to 50 m), but it should help focus our discussion of projectile shape. I refer readers to a paper by Busch *et al.,* 2007) for additional details about asteroid (29075) 1950 DA.

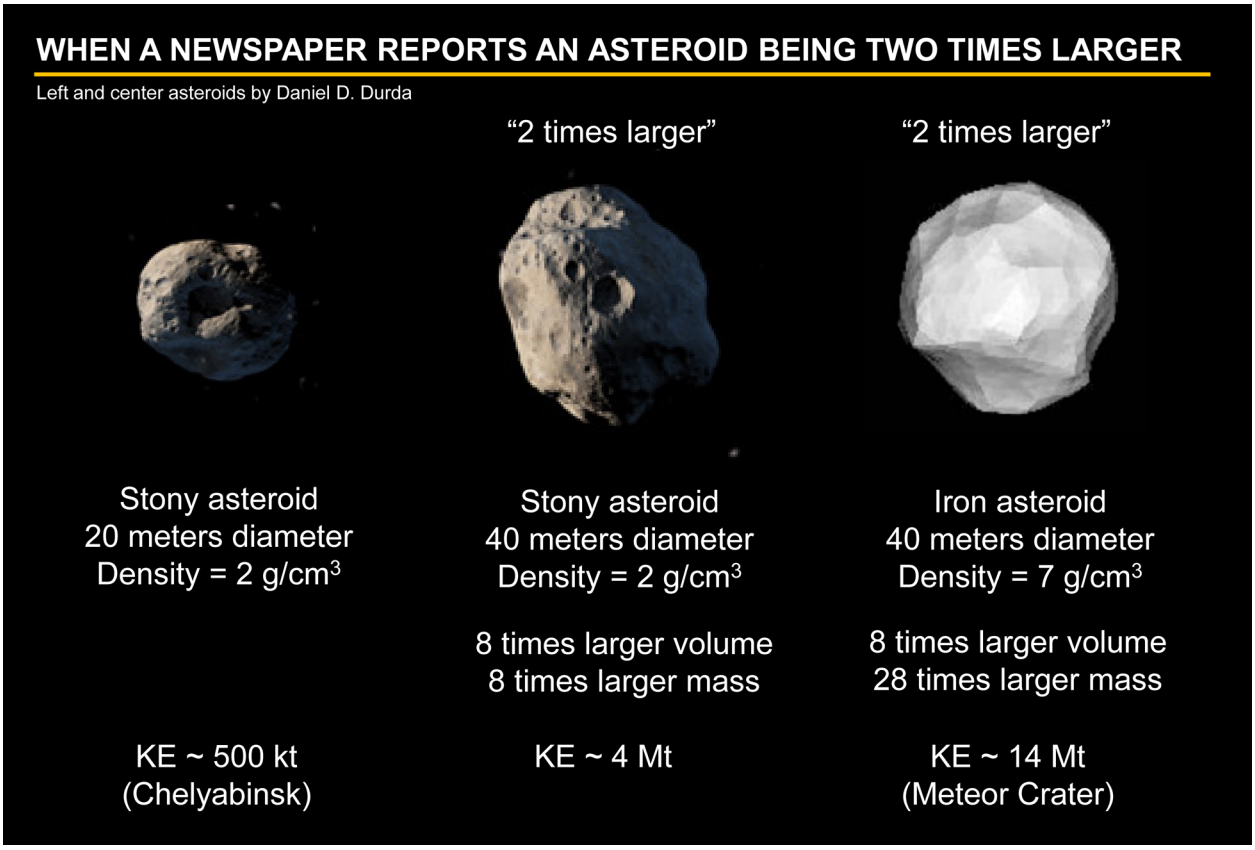

Fig. 9.5. The density of Canyon Diablo meteorite specimens is much higher than that of stony asteroids, like the one that exploded near Chelyabinsk February 15, 2013. That event prompted several comparisons between the Chelyabinsk and Barringer events that did not properly reflect that important property. In news reports, the Chelyabinsk NEA was sometimes described as being half the size of the NEA that produced the famous Meteor Crater in Arizona. That comparison, however, was deceiving, because it did not capture the difference in density and, thus, explosive energy released by the two events. While the NEA that produced Meteor Crater may have been twice the size of the Chelyabinsk NEA, the energy involved was far larger because energy scales with mass, not diameter. The Chelyabinsk NEA was a stony asteroid. A stony asteroid twice that size would have 8 times the volume, mass, and energy of the Chelyabinsk NEA. Meteor Crater was produced by an iron NEA that was much denser. Thus, that NEA, while twice the size and with 8 times the volume, had 28 times more mass and 28 times the kinetic energy of the Chelyabinsk impactor. (Artistic rendering of the two stony NEAs provided by Daniel D. Durda. The iron asteroid is represented by a radar-based shape model of asteroid (29075) 1950 DA that has been dramatically rescaled from 1 km to 40 m for the purpose of this illustration.)

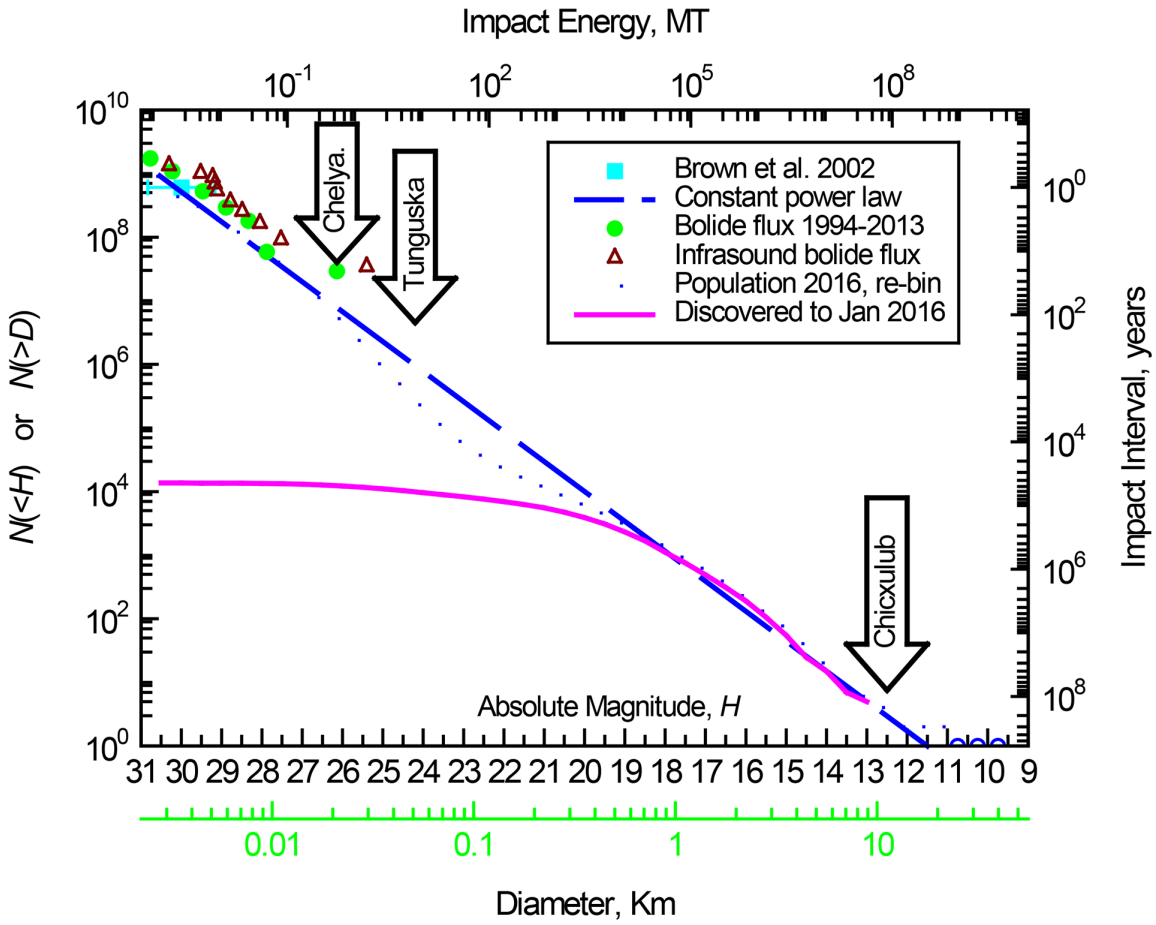

Fig. 9.6. Number (N) of near-Earth objects as a function of absolute magnitude (H) with diameter calculated assuming an average albedo of 0.14 (which makes D = 1 km equivalent to H = 17.75). This is consistent with the average albedo of NEAs measured by NEOWISE. Ancillary scales are provided for average impact interval (right) and for impact energy (top) in MT of equivalent TNT assuming an impact velocity of 20 km/s. For objects the size of the asteroid that produced Barringer Meteorite Crater, there is a large gap between objects detected thus far (magenta curve) and the anticipated population (blue dots and dashed line). For the smaller asteroids, it is important to note that weaker asteroids (dominantly stony asteroids) break up in the atmosphere, as did the Chelyabinsk event of February 15, 2013, while stronger (dominantly iron asteroids) may reach the surface to produce surface explosions and, if on land, a hypervelocity impact crater, like Barringer Meteorite Crater. The diagram appears courtesy of Alan W. Harris (USA) who kindly updated it for this guidebook.

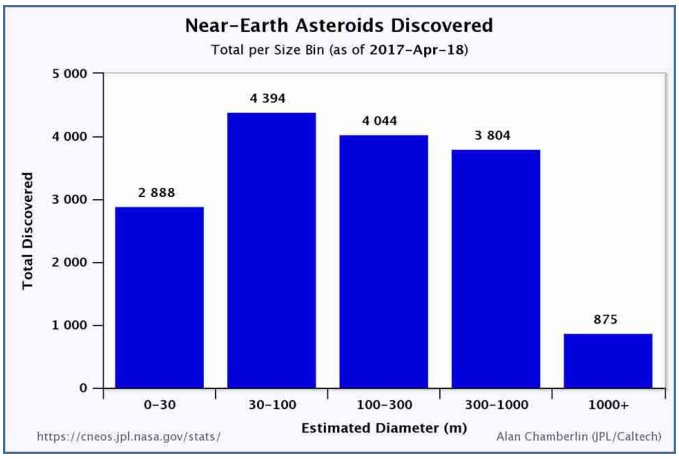

Fig. 9.7. The number of near-Earth asteroids similar in size to the one that produced Barringer Meteorite Crater continues to grow. A few thousand have been discovered thus far: 2,888 in the 0 to 30 m diameter class and 4,394 in the 30 to 100 m diameter class. Data compiled by Alan Chamberlin and current as of April 18, 2017.